doi:10.1038/nature09696

INTRODUCTION

This discussion is organised into three parts. The first presents the mathematical description of the hyperpolarisation sequence applied to the thermal density matrix. The second section introduces the PPT criterion and applies it to derive entanglement thresholds for a selection of preparation strategies. The third section describes the analysis used to collect the final density matrix, error ranges, and a discussion on fidelities.

HYPERPOLARISATION

Si:P is described by an isotropic spin Hamiltonian (in angular frequency units):

$$\mathcal{H}_0 = \omega_e S_z - \omega_I I_z + a \cdot \vec{S} \cdot \vec{I}, \tag{1}$$

where $\omega_e = g\beta B_0/\hbar$ and $\omega_I = g_I \beta_n B_0/\hbar$ are the electron and nuclear Zeeman frequencies, g and g_I are the electron and nuclear g-factors, β and β_n are the Bohr and nuclear magnetons, $\hbar$ is Planck's constant and B_0 is the magnetic field applied along z-axis in the laboratory frame. $S_{x,y,z} = \sigma_{x,y,z} \otimes \mathbb{I}_2$ and $I_{x,y,z} = \mathbb{I}_2 \otimes \sigma_{x,y,z}$.

In the spin basis introduced in the main text, the implementation of the hyperpolarisation sequence upon the first-order Boltzmann thermal state is given by:

$$\begin{aligned}
\rho =& \frac{e^{-\hbar\omega_e S_z/k_B T}}{\mathcal{Z}} \\
=& \frac{1}{\mathcal{Z}} \left(\alpha|1\rangle\langle 1| + \alpha|2\rangle\langle 2| + |3\rangle\langle 3| + |4\rangle\langle 4|\right) \\
\pi_0^{1,3} \rightarrow \rho =& \frac{1}{\mathcal{Z}} (|1\rangle\langle 1| + \alpha|2\rangle\langle 2| + \alpha|3\rangle\langle 3| + |4\rangle\langle 4|) \\
\pi_0^{3,4} \rightarrow \rho =& \frac{1}{\mathcal{Z}} (|1\rangle\langle 1| + \alpha|2\rangle\langle 2| + |3\rangle\langle 3| + \alpha|4\rangle\langle 4|) \\
\tau_{\mathrm{WAIT}} \rightarrow \rho =& \frac{4}{\mathcal{Z}^2} (\alpha|1\rangle\langle 1| + \alpha^2|2\rangle\langle 2| + |3\rangle\langle 3| + \alpha|4\rangle\langle 4|)
\end{aligned} \tag{2}$$

where $\alpha = e^{-\hbar\omega_e/k_B T}$ and $\mathcal{Z} = 2(1+\alpha)$, T is temperature and ω_e the resonant frequency of the electron spin. The ratio of spin-echo amplitudes between the hyperpolarised state to the thermal state on the $|1\rangle$:$|3\rangle$ transition is therefore given by $4/\mathcal{Z} = 2/(\alpha+1)$.

This hyperpolarisation process minimises the linear entropy of the system subject to the available physical processes[1]. Many measures can be used to characterise a state's mixedness; in this work we will use linear entropy because its upper limit for entangled states is tighter

than the von Neumann entropy limit[2]. The linear entropy is given by

$$S_L(\rho) \equiv \frac{\mathcal{N}}{\mathcal{N}-1}[1 - \mathrm{Tr}(\rho^2)] \tag{3}$$

where $\mathcal{N}$ is the dimension of the Hilbert space. The linear entropies of the thermal and hyperpolarised states are given by

$$S_L(\rho_{\mathrm{thermal}}) = \frac{2(1+4\alpha+\alpha^2)}{3(1+\alpha)^2}$$
$$S_L(\rho_{\mathrm{hyperpol}}) = \frac{16\alpha(1+\alpha+\alpha^2)}{3(1+\alpha)^4}$$

The linear entropy decrease is:

$$S_L(\rho_{\mathrm{thermal}}) - S_L(\rho_{\mathrm{hyperpol}}) = \frac{2(1-\alpha)^2(1+\alpha^2)}{3(1+\alpha)^4} \tag{4}$$

ENTANGLEMENT THRESHOLDS

The PPT criterion states that, for a bipartite spin 1/2 system, a state is entangled if and only if its partial transpose has a negative eigenvalue. Explicitly, let us consider a state within the bipartite Hilbert space $\mathcal{H} = \mathcal{H}_A \otimes \mathcal{H}_B$ expressed in the form

$$\rho = \sum_{i,j,k,l} p_{ij,kl} |i\rangle\langle j| \otimes |k\rangle\langle l|$$

where the first pair of indices range over $\mathcal{H}_A$ and the second pair over $\mathcal{H}_B$. The partial transpose of this state is given by

$$\rho^{T_B} = \sum_{i,j,k,l} p_{ij,kl} |i\rangle\langle j| \otimes (|k\rangle\langle l|)^T = \sum_{i,j,k,l} p_{ij,kl} |i\rangle\langle j| \otimes |l\rangle\langle k|.$$

This operation is a transposition of $\mathcal{H}_B$ but not $\mathcal{H}_A$. If a state in $\mathcal{H}$ is a product state, applying such an operation would produce a physically allowed density matrix. Applying the PPT to an entangled state would instead result in an unphysical state, which manifests as a negative eigenvalue. Because $\rho^{T_A} = (\rho^{T_B})^T$, the PPT result does not depend upon which subspace is transposed.

As discussed in the text, our target entangled state was optimally chosen within the limits of the state's linear entropy. We can apply the entangling sequence to the hyperpolarised

state expressed in the form of a density matrix in the $\{|1\rangle, |2\rangle, |3\rangle, |4\rangle\}$ basis.

$$\rho = \frac{4}{\mathcal{Z}^2}\begin{pmatrix} \alpha & 0 & 0 & 0 \\ 0 & \alpha^2 & 0 & 0 \\ 0 & 0 & 1 & 0 \\ 0 & 0 & 0 & \alpha \end{pmatrix}$$

$$\left(\frac{\pi}{2}\right)^{1,3}_{\pi/2}, \pi_0^{3,4} \rightarrow \rho = \frac{2}{\mathcal{Z}^2}\begin{pmatrix} 1+\alpha & 0 & 0 & 1-\alpha \\ 0 & 2\alpha^2 & 0 & 0 \\ 0 & 0 & 2\alpha & 0 \\ 1-\alpha & 0 & 0 & 1+\alpha \end{pmatrix} \tag{5}$$

The partial transpose of this state is:

$$\frac{2}{\mathcal{Z}^2}\begin{pmatrix} 1+\alpha & 0 & 0 & 0 \\ 0 & 2\alpha^2 & 1-\alpha & 0 \\ 0 & 1-\alpha & 2\alpha & 0 \\ 0 & 0 & 0 & 1+\alpha \end{pmatrix}$$

and the eigenvalues of this matrix has a zero crossing when

$$\alpha^3 - (1-\alpha)^2/4 = 0$$

or when $\alpha \approx 0.432$.

It is worth briefly considering the crossing-points for other preparation strategies, in each case using the optimal entangling sequence described above. Three examples include i) the pseudopure preparation scheme applied to the thermal state ii) the thermal state with no preparation and iii) the pseudopure preparation scheme applied to the hyperpolarised state. For i), the prepared pseudopure state has the form

$$\rho_{\mathrm{pp}} = \frac{1}{\mathcal{Z}}\begin{pmatrix} (1+2\alpha)/3 & 0 & 0 & 0 \\ 0 & (1+2\alpha)/3 & 0 & 0 \\ 0 & 0 & 1 & 0 \\ 0 & 0 & 0 & (1+2\alpha)/3 \end{pmatrix}$$

This initial state produces the maximal amount of entanglement when arranged in the form

equivalent under local unitaries to

$$\rho_{\rm pp} = \frac{1}{\mathcal{Z}} \begin{pmatrix} (4+2\alpha)/6 & 0 & 0 & (2-2\alpha)/6 \\ 0 & (1+2\alpha)/3 & 0 & 0 \\ 0 & 0 & (1+2\alpha)/3 & 0 \\ (2-2\alpha)/6 & 0 & 0 & (4+2\alpha)/6 \end{pmatrix}$$

The partial transpose of this matrix has a zero crossing when

$$2\alpha + \alpha^2 = 0$$

and so the only 'physical' zero crossing occurs at $\alpha = 0$. Of course, these calculations assume that the nuclear spin polarisation is negligible; in the regime of $\alpha \approx 0$ the polarisation of the nucleus would have to be considered in this calculation. This would allow for a small but nonzero threshold for α, dependent upon the nuclear spin isotope.

For ii), the maximally entangled state is equivalent under local unitaries to

$$\rho_{\rm pp} = \frac{1}{\mathcal{Z}} \begin{pmatrix} (1+\alpha)/2 & 0 & 0 & (1-\alpha)/2 \\ 0 & \alpha & 0 & 0 \\ 0 & 0 & 1 & 0 \\ (1-\alpha)/2 & 0 & 0 & (1+\alpha)/2 \end{pmatrix}$$

The partial transpose of this matrix has a positive zero crossing when $\alpha = -3 + 2\sqrt{2}$, so entanglement is possible below $\alpha \approx 0.17$.

For iii), the maximally entangled state is equivalent under local unitaries to

$$\rho_{\rm pp} = \frac{4}{\mathcal{Z}^2} \begin{pmatrix} (3+2\alpha+\alpha^2)/6 & 0 & 0 & (3-2\alpha-\alpha^2)/6 \\ 0 & \alpha(2+\alpha)/3 & 0 & 0 \\ 0 & 0 & \alpha(2+\alpha)/3 & 0 \\ (3-2\alpha-\alpha^2)/6 & 0 & 0 & (3+2\alpha+\alpha^2)/6 \end{pmatrix}$$

The partial transpose of this matrix has a positive zero crossing when $\alpha = \sqrt{2} - 1$, and so entanglement is possible below $\alpha \approx 0.4142$.

DENSITY MATRIX CALCULATIONS

We used phase (Z) rotations to probe the existence of coherences without disturbing the state populations, which were measured separately by mapping pairs of population differences into the S_x observable. In typical electron spin resonance experiments, phase rotations

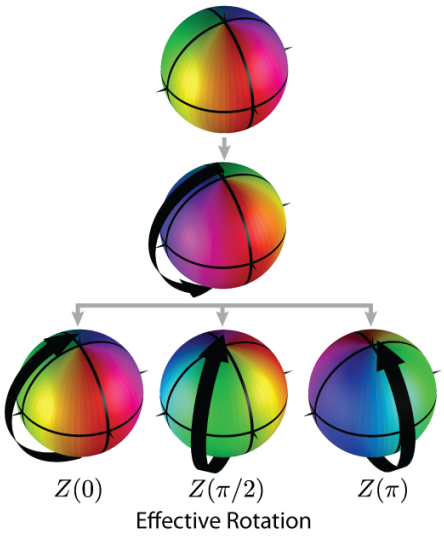

FIG. 1: **Geometric Phase Rotations** Geometric Z-gates can be applied to a single spin using two consecutive π pulses along different axes. The black arrows at each step illustrate the applied rotation to the Bloch sphere, and the colouring displays this rotation. Three sample geometric Z-gate rotations are shown along the bottom.

are not directly available operations; they can be implemented with various strategies including the use of off-resonant pulses and appropriate delays, phase-shifted final reference frames[3] and composite rotations made up of pure X and Y rotations of variable length[4]. In this work, we follow an approach inspired by the Aharonov-Anandan geometric phase gate[5] and apply two selective MW or RF π pulses of differing phases. Given the larger Hilbert space of this two-spin system, and the fact that we are applying selective rotations that cannot be understood in terms of the independent manipulation of either spin, the most instructive way to appreciate the effect of this gate is to examine the phase acquired by each eigenstate under the rotation (see Figure 2 of the main text). However, for a single spin 1/2, the same gate has a convenient visual representation that is illustrated in Figure 1 in terms of the rotation of the Bloch sphere.

To calculate the final density matrix we first constructed the pseudo-pure density matrix. A baseline measurement was taken as an average of 2000 samples, and all datasets were baseline-corrected before processing. The population differences were measured by an average of 100 samples and scaled with respect to a measured thermal amplitude (also taken

as an average over 100 samples), and adjusted to have unit trace with the addition of an appropriately scaled identity matrix.

The coherence-measurement pulse sequences were all individually tested by verifying their output frequencies when applied to their target coherences. Upper diagonal elements were gathered and their conjugate values populated the lower diagonal elements. The coherences were collected with 128 points and baseline-corrected before being Fourier transformed and normalised with respect to the thermal amplitude. A narrow integral over the appropriate frequency position was made to measure the coherences. The frequencies were chosen such that all frequency peaks were well-resolved with a 128-point Fourier transform.

The calculated pseudopure matrix $\rho_{\rm pp}$ was added to the appropriate amount of identity matrix $\mathbb{I}$ as determined by a spin-temperature measurement, where $e^{-\hbar\omega_s/k_bT} = \alpha \leq 0.217$. The explicit reconstruction is given by

$$\rho_F = [\alpha/(2(1+\alpha))]\mathbb{I} + [(1-\alpha)/((1+\alpha))]\rho_{\rm pp}$$

There are two conventional measures[6,7] of state fidelity, $\mathcal{F}(\rho_1,\rho_2) = \left(\mathrm{Tr}\left(\sqrt{\sqrt{\rho_2}\rho_1\sqrt{\rho_2}}\right)\right)^2$ or alternatively the more generous measure $\sqrt{\mathcal{F}(\rho_1,\rho_2)}$. When applied to physically allowed states, both measures are non-negative and reach a maximum value of 1 when $\rho_1 = \rho_2$. The fidelity used in the main text calculates $\mathcal{F}$ when comparing the gathered density matrix with the target density matrix (calculated by Equation 5 with $\alpha = 0.217$). This measure yields a fidelity of 0.982(2), while the often-used alternative measure $\sqrt{\mathcal{F}}$ displays a fidelity of 0.991(2) with the target state. We can also compare the gathered density matrix to the ideal Bell state $\rho_B = \frac{1}{\sqrt{2}}(|00\rangle\langle 00| + |11\rangle\langle 11|)$ given by Equation 5 with $\alpha = 0$. The adopted fidelity $\mathcal{F}$ reveals a fidelity of 0.68(2), while the more generous $\sqrt{\mathcal{F}}$ produces a fidelity of 0.82(1) with the pure Bell state.

The errors corresponding to each density matrix element were calculated according to the standard error of the measurement taken. For the populations this consisted of the standard error of the direct difference measurements; for the coherences this consisted of the standard error of the Fourier-transformed signal over the integral peak width. These density matrix element errors were transformed into final negativity, concurrence and fidelity errors by Monte Carlo generation of density matrices. The generated matrices deviated from the measured matrix in each element by an amount chosen randomly from a normal distribution whose standard deviation matched that elements' error. Once re-normalised, unphysical

matrices were discarded and statistics on physical matrices were collected. In total, 2^{12} matrices were used to compile the final errors.

[1] Schulman, L. J., Mor, T. & Weinstein, Y. Physical Limits of Heat-Bath Algorithmic Cooling. *Phys. Rev. Lett.* **94** (2005).

[2] Wei, T.-C. Maximal entanglement versus entropy for mixed quantum states. *Phys. Rev. A* **67** (2003).

[3] Mehring, M., Mende, J. & Scherer, W. Entanglement between an Electron and a Nuclear Spin 1/2. *Phys. Rev. Lett.* **90**, 153001 (2003).

[4] Suter, D., Mueller, K. T. & Pines, A. Study of the Aharonov-Anandan quantum phase by NMR interferometry. *Phys. Rev. Lett.* **60**, 1218–1220 (1988).

[5] Aharonov, Y. & Anandan, J. Phase change during a cyclic quantum evolution. *Phys. Rev. Lett.* **58**, 1593–1596 (1987).

[6] Jozsa, R. Fidelity for mixed quantum states. *Journal of Modern Optics* (1994).

[7] DiCarlo, L. *et al.* Demonstration of two-qubit algorithms with a superconducting quantum processor. *Nature* **460**, 240–244 (2009).